

How individual species structure diversity in tropical forests

Thorsten Wiegand*[†], C. V. Savitri Gunatilleke[‡], I. A. U. Nimal Gunatilleke[‡], and Andreas Huth*

*Department of Ecological Modeling, UFZ Helmholtz Centre for Environmental Research-UFZ, PF 500136, D-04301 Leipzig, Germany; and [‡]Faculty of Science, Department of Botany, University of Peradeniya, Peradeniya 20400, Sri Lanka

Edited by Simon A. Levin, Princeton University, Princeton, NJ, and approved October 15, 2007 (received for review June 20, 2007)

A persistent challenge in ecology is to explain the high diversity of tree species in tropical forests. Although the role of species characteristics in maintaining tree diversity in tropical forests has been the subject of theory and debate for decades, spatial patterns in local diversity have not been analyzed from the viewpoint of individual species. To measure scale-dependent local diversity structures around individual species, we propose individual species–area relationships (ISAR), a spatial statistic that marries common species–area relationships with Ripley’s K to measure the expected α diversity in circular neighborhoods with variable radius around an arbitrary individual of a target species. We use ISAR to investigate if and at which spatial scales individual species increase in tropical forests’ local diversity (accumulators), decrease local diversity (repellers), or behave neutrally. Our analyses of data from Barro Colorado Island (Panama) and Sinharaja (Sri Lanka) reveal that individual species leave identifiable signatures on spatial diversity, but only on small spatial scales. Most species showed neutral behavior outside neighborhoods of 20 m. At short scales (<20 m), we observed, depending on the forest type, two strongly different roles of species: diversity repellers dominated at Barro Colorado Island and accumulators at Sinharaja. Nevertheless, we find that the two tropical forests lacked any key species structuring species diversity at larger scales, suggesting that “balanced” species–species interactions may be a characteristic of these species-rich forests. We anticipate our analysis method will be a starting point for more powerful investigations of spatial structures in diversity to promote a better understanding of biodiversity in tropical forests.

biodiversity | spatial patterns | spatial statistic | species–area relationship

Since the establishment of large permanent sampling plots where all stems >1 cm in diameter at breast height (dbh) are identified, measured, and mapped (1, 2), substantial progress has been made in explaining the high local diversity of tree species in tropical forests; however, ecologists are still far from having a definitive answer. Several competing hypotheses on processes promoting species coexistence have been developed and tested, but these efforts have yielded contrasting results (3–5). Neutral theory (6–8) suggested that species-specific differences are unimportant for certain community attributes, whereas niche theory outlines the importance of species characteristics and trade-offs (9, 10). It is also clear that species-specific differences affect the spatial distribution of populations (11–16). Surprisingly, although plant–plant interactions should play a major role in structuring tropical forests, the resulting spatial patterns in diversity have not been analyzed from the viewpoint of individual species. However, strong differences in species traits and in species interactions should create clearly identifiable nonrandom spatial structures in diversity that would not arise for neutral species.

Here, we propose the framework of individual species–area relationships (ISAR) to study species-specific effects on local diversity in species-rich communities. The $ISAR(a)$ function is the expected number of species within circular areas $a = \pi r^2$ around an arbitrary individual of a target species where r is the

radius of the neighborhood area a . ISAR is a statistic to analyze the spatial diversity structure in forest ecosystems and reconciles common species–area relationships (17–19) and the individual perspective of point-pattern analysis (20–22).

The ISAR allows for a subtle assessment of species effects on local diversity with respect to their interactions with plants of other species. If positive facilitative interactions with other species dominate, the target species would accumulate and maintain an overrepresentative proportion of diversity in its proximity (i.e., being a “diversity accumulator”). In instances where negative interactions dominate, the target species tolerates only an underrepresentative proportion of other species in its neighborhood (i.e., a “diversity repeller”). However, if positive and negative interactions are weak or even out, the species behaves neutrally.

Note that species interactions are not the only factors that may influence the ISAR; the spatial pattern of the target species (i.e., clustering or overdispersion) and habitat associations may also produce ISAR curves of the accumulator or repeller type. The effect of dispersion is important for interpreting and understanding ISAR but can be diagnosed by comparing local densities of the stems of the target species with that of all species in neighborhoods around the stems of the target species [see supporting information (SI) Table 1]. A species may appear to be a diversity accumulator or repeller through habitat association if diversity differs at different habitats [e.g., upper and lower elevation habitats at Sinharaja (23)]. This effect is analogous to the problem of heterogeneous patterns in point-pattern analysis (21, 24). Specific methods are required to factor out the effects of habitat association [i.e., a “heterogeneous” null model (24); see *Null Models of Neutral Species*]. To accomplish this, we used Monte Carlo simulations of the heterogeneous null model of a neutral species to assess if a species is a significant diversity accumulator, repeller, or neutral and at what spatial scales.

Assessment of the proportion of diversity accumulator, repellers, and neutral species at different spatial scales provides important insights into the spatial structures of species-rich communities, its critical spatial scales, and allows testing how many species in a community behave neutrally with respect to the spatial patterns. Studies investigating neighborhood effects on tree growth and survival showed that direct plant–plant interactions are strong at local plant neighborhoods (of, say, <30 m) but fade away at larger scales (12–14, 25). We therefore expect strong departures from a neutral ISAR at local neighborhoods but mostly neutral ISARs at larger scales.

Author contributions: T.W. and A.H. designed research; T.W., C.V.S.G., I.A.U.N.G., and A.H. performed research; T.W. analyzed data; and T.W., C.V.S.G., I.A.U.N.G., and A.H. wrote the paper.

The authors declare no conflict of interest.

This article is a PNAS Direct Submission.

[†]To whom correspondence should be addressed. E-mail: thorsten.wiegand@ufz.de.

This article contains supporting information online at www.pnas.org/cgi/content/full/0705621104/DC1.

© 2007 by The National Academy of Sciences of the USA

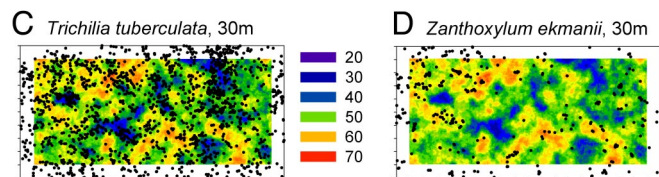
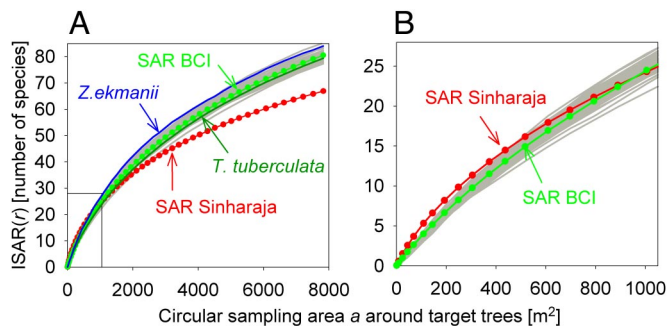


Fig. 1. Individual species–area relationships at BCI from the 1995 census. (A) The empirical ISAR for the 63 most-common species (gray solid lines) and for two example species (blue and dark green lines). The green and red circles show the common SAR for BCI and Sinharaja, respectively. (B) Enlargement of A for small scales, $r < 18$ m. Symbols as in A. (C) Spatial pattern of the species *Trichilia tuberculata* together with the underlying distribution of local species diversity at 30-m neighborhoods (plot size, $1,000 \times 500$ m; see also SI Fig. 7). The local diversity in 30-m neighborhoods ranged from 25 to 60 species. (D) Same as C for the species *Zanthoxylum ekmanii*.

We applied this framework to data from two fully censused 50- and 25-ha tree plots at Barro Colorado Island (BCI), Panama (26, 27), and Sinharaja, Sri Lanka (23, 28), respectively. We selected these two sites because they constitute two extremes with respect to habitat association among the Forest Dynamics Plots coordinated within the network of the Centre for Tropical Forest Science (CTFS); the Sinharaja plot shows high species–habitat associations (23) and the BCI plot shows low species–habitat associations (29). We derive the empirical ISAR curves of abundant tree species with dbh > 10 cm and investigate (i) if the spacing of trees retains a signature of species “individuality” with respect to local diversity, (ii) if species act as diversity accumulators, repellers, or behave neutrally, and (iii) to what extent and at which spatial scales these species attributes, if present, might be caused by species interactions or by larger-scale habitat association.

Results

Our analysis shows that the ISAR curves were remarkably similar at BCI and did not depart by more than ± 4 species from the common species–area relationship (SAR) (Fig. 1A). Interestingly, the SAR was at larger scales well within the range of ISARs occurring at the BCI plot (Fig. 1A) and practically indistinguishable from the average of all ISARs measured (SI Fig. 4A and B). Thus, there were no key species that strongly structured the community spatially. The variability in the ISAR curves at BCI, measured as the difference between the maximal and minimal ISAR at scale r , increased linearly up to a scale of 30 m before reaching a maximum of ≈ 8 species (SI Fig. 5).

In the next step, we roughly assessed scale-dependent effects. To determine the proportion of accumulators or repellers, we counted at each scale r the number of species for which the empirical $ISAR(r)$ was $> 97\%$ or $< 3\%$ of the simulated $ISAR(r)$, respectively. For BCI, we found large proportions of diversity repellers at neighborhoods closer than 10 m which, however, disappeared at neighborhoods of ≈ 20 m (Fig. 3A). Interestingly, at BCI, there were almost no diversity accumulators (Fig. 3A).

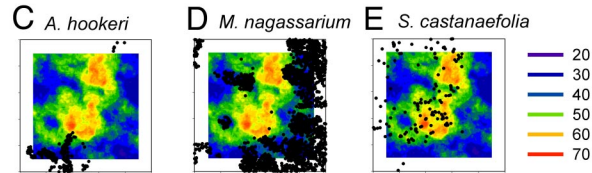
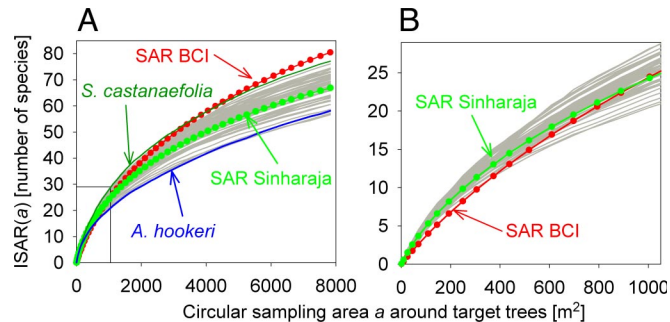


Fig. 2. Individual species–area relationships at Sinharaja from the 1995 census. (A) The empirical ISAR for the 47 most-common species (gray solid lines) and for two example species (blue and dark green lines). The green and red circles show the common SAR for Sinharaja and BCI, respectively. (B) Enlargement of A for small scales, $r < 18$ m. Symbols as in A. (C) Spatial pattern of the species *Agrostistachys hookeri* together with the underlying local diversity within 30-m neighborhoods which ranged from 23 to 68 species (plot size, 500×500 m; also see SI Fig. 7). (D) Same as C for the species *Mesua nagassarium*. (E) Same as C for species *Schumacheria castaneaefolia*.

Fig. 3A indicates that significant effects were only likely to occur in neighborhoods of < 20 m. We therefore used a goodness-of-fit test with α level of 0.05 to assess the overall fit of the empirical ISAR curves with the heterogeneous null model over scales $r = 0–20$ m. This test revealed that 65% of all species at BCI behaved neutrally. We found no clear trends when relating the property repeller or accumulator to a common tree species classification (30), large tree species were slightly overrepresented among the accumulators, and midsize trees were slightly underrepresented among the repellers (SI Fig. 6A).

As expected because of the larger habitat heterogeneity of the Sinharaja plot, the empirical ISAR curves showed larger differences than those at BCI (compare Figs. 2A and 1A). The variability in the ISAR curves increased almost linearly to a value of ≈ 20 at the 50-m scale without reaching a plateau as found at BCI (SI Fig. 5). This increase is probably due to the two clearly identifiable areas of below- and above-average diversity that appear at Sinharaja if the number of species is counted in neighborhoods > 30 m (see SI Fig. 7). Again, the SAR was practically indistinguishable from the average of all ISARs measured (SI Fig. 4A and B). When looking at scale effects, we found a pattern that markedly differed from that at BCI: only few species were diversity repellers, but diversity accumulators were more frequent (Fig. 3B). Fig. 3B shows that significant effects occurred only in neighborhoods of < 20 m. When testing the overall fit of the empirical ISAR curves with the heterogeneous null model over scales $r = 0–20$ m, we found that 75% of all species at Sinharaja behaved neutrally. At Sinharaja, accumulators were slightly underrepresented in the canopy species class but overrepresented in the subcanopy species class, and repellers were slightly overrepresented in the canopy species class but underrepresented in the subcanopy species class (SI Fig. 6B).

Discussion

Using data on the bivariate spatial patterns of hundreds of species in two contrasting forest dynamics plots in Sri Lanka and Panama, we found that species-specific effects on local diversity were surprisingly low and limited to the canopy range or

that $\approx 30\%$ of the species at BCI showed significant affinities to soil nutrient distributions.

We hypothesize that the weak species-specific effects on local diversity found in our study should be related to the high diversity of tropical forests. What would happen if species effects on biodiversity were stronger? In absence of pronounced habitat structure, a strong diversity repeller would have a tendency to generate monospecific or low-diversity patches and would introduce considerable instability into the community dynamics. Such species would function similarly to aggressive invaders, reducing species diversity. Strong diversity accumulators, on the other hand, are difficult to imagine in tropical forests but may be more common in harsh environments where they modify their environment, making it more benign for other species. It would be interesting to expand our analysis to species-poorer forests, for example temperate forests, to find out if and to what extent the strength and proportion of repellers and accumulators are related to tree-species richness. ISAR is a spatial statistic that describes spatial diversity patterns in fully mapped tree census plots in a simple and intuitive way by marrying the well established species–area relationships with Ripley’s K . We are just beginning to explore the features and the power of this framework and are confident that it will shed new light on the role of plant–plant interactions in maintaining tree diversity in tropical forests.

Methods

Study Sites. The study was carried out in two tropical forests at BCI, Panama ($9^{\circ}10'N$, $79^{\circ}51'W$), and Sinharaja, Sri Lanka ($6^{\circ}21'–26'N$, $80^{\circ}21'–34'E$). The forest at BCI is a seasonally moist tropical forest, and rainfall averages 2,600 mm per year with a pronounced dry season. Investigations were carried out within the Forest Dynamics Project 50-ha plot, which consists of mainly old growth lowland moist forest. Elevation ranges from 120 to 155 m above mean sea level. The plot was established in 1982, and all trees >1 cm dbh have been mapped, tagged, and measured every 5 years since 1985. Based on the 1995 census, there are at BCI, on average, ≈ 0.5 , ≈ 0.042 , ≈ 0.016 , and ≈ 0.005 stems per m^2 with dbh >1 cm, >10 cm, >20 cm, and >50 cm, respectively. Thus, an average stem with dbh >10 cm covers an area of $\approx 23.8m^2$, which corresponds to a circular area with a radius of 2.8 m. Details on the plot are provided in refs. 1 and 2.

The 25-ha plot at Sinharaja is a tropical forest without a regular dry season, and rainfall averages 5,016 mm per year. Elevation ranges from 424 to 575 m above mean sea level and includes a valley lying between two slopes. Tree species show varying degree of associations to habitat types defined by topography. The Sinharaja plot was established in 1993, and all trees >1 cm dbh have been mapped, tagged, and measured. At Sinharaja, there are, on average, ≈ 0.8 , ≈ 0.067 , ≈ 0.028 , and ≈ 0.004 stems per m^2 with dbh >1 cm, >10 cm, >20 cm, and >50 cm, respectively. Every stem with dbh >10 cm covers, on average, an area of $\approx 14.9 m^2$, which corresponds to a circular area with a radius of 2.2 m. Details on the plot are provided in refs. 23 and 28. In the present analysis, we used data on trees with dbh >10 cm from the third (1995) BCI census (26, 27) and from the first (1994–1996) Sinharaja census.

Definition and Estimation of ISAR. To find out if and at what spatial scales a given species has a significant effect on diversity, we needed to measure the relationship between the spatial pattern of plants of the target species and the pattern of the plants of the other species of the community and compare it to a null model of a neutral species. Although established techniques of point-pattern analysis that are able to assess association between pairs of species (21, 22) could potentially be used for this purpose, this becomes a very tedious task if many species are involved (22),

and the results of the many individual analyses cannot be summarized effectively on the community (diversity) level.

We therefore developed an analogous approach of point-pattern analysis that does not work at the species–species level but on the species–community level. Whereas Ripley’s bivariate K -function measures at the species–species level the number of stems of one species up to distance r away from an arbitrary stem of a target species, our measure, the ISAR, measures at the species–community level the number of species up to distance r away from an arbitrary stem of the target species. Our framework is thus located intermediate between conventional SARs (17) that summarize the diversity of a community in a scale-dependent manner but which do not provide a direct link to species–species interactions and studying species–species relationships with bivariate point-pattern analysis (22).

To estimate the $ISAR(r)$, the expected number of species within circular areas with radius r around an average individual of the target species t , we first calculated the bivariate emptiness probability $P_{ij}(0, r)$ that species j was not present in the circles with radius r around the trees of the target species t (note that we do not count the focal stem if $t = j$) and then summed up $1 - P_{ij}(0, r)$ for all species present in the plot:

$$ISAR(r) = \sum_{j=1}^N [1 - P_{ij}(0, r)].$$

Using $a = \pi r^2$, we can express the ISAR also in terms of area a , to resemble the common species–area relationship. Because the $P_{ij}(0, r)$ are derived from the bivariate pattern of species j and t , the ISAR contains information about all interspecific spatial patterns, but on a highly aggregated level. To avoid sample circles of target stems located close to the border of the plot not being located entirely inside the census plot, we used edge correction with a buffer zone. For this purpose, only stems of the target species t within an inner plot were used to determine the bivariate emptiness probabilities $P_{ij}(0, a)$, whereas all stems of species j in the entire plot were used. Consequently, ISAR can only be calculated for spatial scales up to the width of the buffer zone.

To work with reasonable sample sizes, we estimated the ISAR only for species having >70 individuals, yielding 63 species at BCI and 47 at Sinharaja. To cover the range of scales where tree–tree interactions, effects of dispersal limitation, or succession in light gap are most likely to occur, we calculated all scale-dependent function up to a maximal scale of $r_{max} = 50$ m with steps of 1 m. Consequently, we selected a buffer zone width of 50 m.

Null Models of Neutral Species. To test if a given species is a significant diversity accumulator, a significant diversity repeller, or if the species behaved neutrally, we performed Monte Carlo simulations of null models by using ISAR as test statistic. The simplest null model randomizes the locations of the trees of the target species (“homogeneous Poisson” null model), thereby removing the potential effects of interactions with individuals of other species on its spatial distribution (i.e., removing “second-order effects”). However, in point-pattern analysis, it is recognized that the outcome of analyses with the homogeneous Poisson null model may be confounded by “first-order effects” (21, 24) where habitat association increases or decreases the likelihood that an individual will occur at a given location. We therefore used a heterogeneous Poisson null model (22, 24, 37) in which the individuals of the target species are distributed in accordance with the (spatially variable) intensity of the target species. We estimated the intensity function by using an Epanechnikov kernel with a bandwidth of 50 m (*SI Text*), which removes all potential spatial structure in the pattern of the target

species at scales <50 m but maintains the spatial structure at scales >50 m. This null model thus factors out first-order effects and allows a proper examination of the second-order effects. Note that this approach is based on a separation of scales. Several studies using individual-based analyses of local neighborhood effects on growth and survival have shown that direct plant–plant interactions may operate only at local plant neighborhoods <20 – 30 m, fading away at larger scales (12–14, 25), and the parameter σ of dispersal kernels at BCI typically range at approximately $\sigma < 40$ – 50 m ($2\sigma^2$ is the mean square dispersal distance from parent to surviving offspring) (38). On the other hand, habitat conditions for trees, i.e., elevation, orientation, or soil nutrients, vary typically at larger scales along environmental gradients that are often related with topographical features such as slope and elevation (22, 23, 29, 36). Details on the implementation and computer code of the heterogeneous Poisson null model are given in the *SI Text*.

Note that the ISAR of a randomly distributed species corresponds to the conventional species–area relationship with randomly distributed circular sampling units instead of the conventionally used nested disjoint rectangular sampling units. For the relatively small neighborhoods analyzed here (<1 ha) compared with the plot sizes (25 and 50 ha), the random sampling approximates the SAR well.

Statistical Inference. To assess effects at different scales r , we followed the common practice in point-pattern analysis and constructed Monte Carlo simulation envelopes based on the 99 simulations of the two null models. If the empirical $ISAR(r)$ was at a given scale r larger than the second highest $ISAR(r)$ of all 99 simulations of the null model, the species was regarded at scale r as a diversity accumulator with an approximate α level of 0.05. Conversely, if the empirical $ISAR(r)$ was at a given scale r smaller than the second smallest $ISAR(r)$ of all 99 simulations, the species was regarded at scale r as a diversity repellent. If the empirical $ISAR(r)$ was within the range of the null model, the species was

considered neutral at scale r . However, because of simultaneous inference, the simulation envelopes cannot be interpreted as confidence intervals (39); the type I error (i.e., a neutral species is regarded as accumulator or repeller) is $>5\%$. Thus, our estimates of the proportion of neutral species at different scales r are conservative.

To avoid the problem of simultaneous inference, we additionally used a goodness-of-fit test (21, 39) that assessed the overall fit of the empirical ISAR curves with a given null model over a range of scale of interest. This range was the range of scales where significant departures from the simulation envelopes occurred frequently for the species tested, i.e., $r = 0, \dots, 20$ m for the heterogeneous null model (Fig. 3A) and $r = 0, \dots, 50$ m for the homogeneous null model (SI Fig. 8). Under this test, both the observed $ISAR(r)$ for all scales r of interest and each of the 99 Monte Carlo simulated ISARs of a given null model are reduced to a single summary test statistic that represents the total squared deviation between the observed ISAR and the theoretical ISAR across the distances of interest. If the summary statistic computed for the observed ISAR was larger than that of the fifth largest of the 99 simulated ISAR, then the observed ISAR was regarded to differ significantly from a neutral ISAR with an α level of 0.05.

The Forest Dynamics Plots of Barro Colorado Island and Sinharaja have been made possible through the generous support of the United States National Science Foundation, The John D. and Catherine T. MacArthur Foundation, the Smithsonian Tropical Research Institute, the Centre for International Development at Harvard University, and through the hard work of over 100 people from 10 countries over the past two decades. The BCI and Sinharaja Forest Dynamics Plots are part of the Center for Tropical Forest Science, a global network of large-scale demographic tree plots. We thank the permission given to work in Sinharaja World Heritage Site and the accommodation facilities provided by the Forest Department of Sri Lanka as well as the contributions of the National Institute for Environmental Studies, Japan, for the first and second censuses at Sinharaja. The manuscript benefited from comments by J. Grönfeld, Justin Calabrese, and two anonymous reviewers.

- Condit R (1998) *Tropical Forest Census Plots* (Springer, Berlin).
- Losos EC, Leigh EG (2004) *Tropical Forest Diversity and Dynamism* (University of Chicago Press, Chicago).
- Wright SJ (2002) *Oecologia* 130:1–14.
- Hubbell SP (2004) in *Tropical Forest Diversity and Dynamism: Findings from a Large-Scale Plot Network*, eds Losos EC, Leigh EG (University of Chicago Press, Chicago), pp 8–30.
- Köhler P, Huth A (2007) *Ecol Modell* 203:511–517.
- Hubbell SP (2001) *The Unified Neutral Theory of Biodiversity and Biogeography* (Princeton Univ Press, Princeton).
- Volkov I, Banavar JR, He F, Hubbell SP, Maritan A (2005) *Nature* 438:658–661.
- Chave J (2004) *Ecol Lett* 7:241–253.
- Tilman D (2004) *Proc Natl Acad Sci USA* 101:10854–10861.
- Baker PJ, Wilson JS (2003) *Nature* 422:581–582.
- Lortie CJ, Brooker RW, Choler P, Kikvidze Z, Michalet R, Pugnaire FI, Callaway RM (2004) *Oikos* 107:433–438.
- Stoll P, Newbery DM (2005) *Ecology* 86:3048–3062.
- Hubbell SP, Ahumada JA, Condit R, Foster RB (2001) *Ecol Res* 16:859–875.
- Peters HA (2003) *Ecol Lett* 6:757–765.
- Condit R, Ashton P, Bunyavejchewin S, Dattaraja HS, Davies S, Esufali S, Ewango C, Foster R, Gunatilleke IAUN, Gunatilleke CVS, et al. (2006) *Science* 313:98–101.
- Harms KE, Wright SJ, Calderon O, Hernandez A, Herre EA (2000) *Nature* 404:493–495.
- He FL, Legendre P (2002) *Ecology* 83:1185–1198.
- Plotkin JB, Potts MD, Yu DW, Bunyavejchewin S, Condit R, Foster R, Hubbell S, LaFrankie J, Manokaran N, Seng LH, et al. (2000) *Proc Natl Acad Sci USA* 97:10850–10854.
- Plotkin JB, Potts MD, Leslie N, Manokaran N, LaFrankie J, Ashton PS (2000) *J Theor Biol* 207:81–99.
- Lieberman M, Lieberman D (2007) *Oikos* 116:377–386.
- Diggle PJ (2003) *Statistical Analysis of Spatial Point Patterns* (Hodder Arnold, London).
- Wiegand T, Gunatilleke CVS, Gunatilleke IAUN (2007) *Am Nat* 170:E77–E95.
- Gunatilleke CVS, Gunatilleke IAUN, Esufali S, Harms KE, Ashton PMS, Burslem DFRP, Ashton PS (2006) *J Trop Ecol* 22:371–384.
- Wiegand T, Moloney KA (2004) *Oikos* 104:209–229.
- Uriarte M, Condit R, Canham CD, Hubbell SP (2004) *J Ecol* 92:348–360.
- Condit R, Hubbell SP, Foster RB *Barro Colorado Forest Census Plot Data*. Available at <http://ctfs.si.edu/datasets/bci>. Accessed September 1, 2006.
- Hubbell SP, Foster RB, O'Brien ST, Harms KE, Condit R, Wechsler B, Wright SJ, de Lao SL (1999) *Science* 283:554–557.
- Gunatilleke CVS, Gunatilleke IAUN, Ethugala AUK, Esufali S (2004) *Ecology of Sinharaja Rain Forest and the Forest Dynamics Plot in Sri Lanka's Natural World Heritage Site* (WHT Publications, Colombo, Sri Lanka).
- Harms KE, Condit R, Hubbell SP, Foster RB (2001) *J Ecol* 89:947–959.
- Condit R, Hubbell SP, Foster RB (1996) *J Trop Ecol* 12:231–256.
- Condit R, Hubbell SP, LaFrankie JV, Sukumar R, Manokaran N, Foster RB, Ashton PS (1996) *J Ecol* 84:549–562.
- McGill BJ (2003) *Nature* 422:881–885.
- Clark JS, McLachlan JS (2003) *Nature* 423:635–638.
- Hubbell SP (2005) *Funct Ecol* 19:166–172.
- McGill BJ, Maurer BA, Weiser MD (2006) *Ecology* 87:1411–1423.
- John R, Dalling JW, Harms KE, Yavitt JB, Stallard RF, Mirabello M, Hubbell SP, Valencia R, Navarrete H, Vallejo M, et al. (2007) *Proc Natl Acad Sci USA* 104:864–869.
- Stoyan D, Stoyan H (1994) *Fractals, Random Shapes and Point Fields* (Wiley, New York).
- Condit R, Pitman N, Leigh EG, Chave J, Terborgh J, Foster RB, Nunez P, Aguilar S, Valencia R, Villa G, et al. (2002) *Science* 295:666–669.
- Loosmore NB, Ford ED (2006) *Ecology* 87:1925–1931.

Supporting Information

Files in this Data Supplement:

[SI Table 1](#)

[SI Figure 4](#)

[SI Figure 5](#)

[SI Figure 6](#)

[SI Figure 7](#)

[SI Figure 8](#)

[SI Text](#)

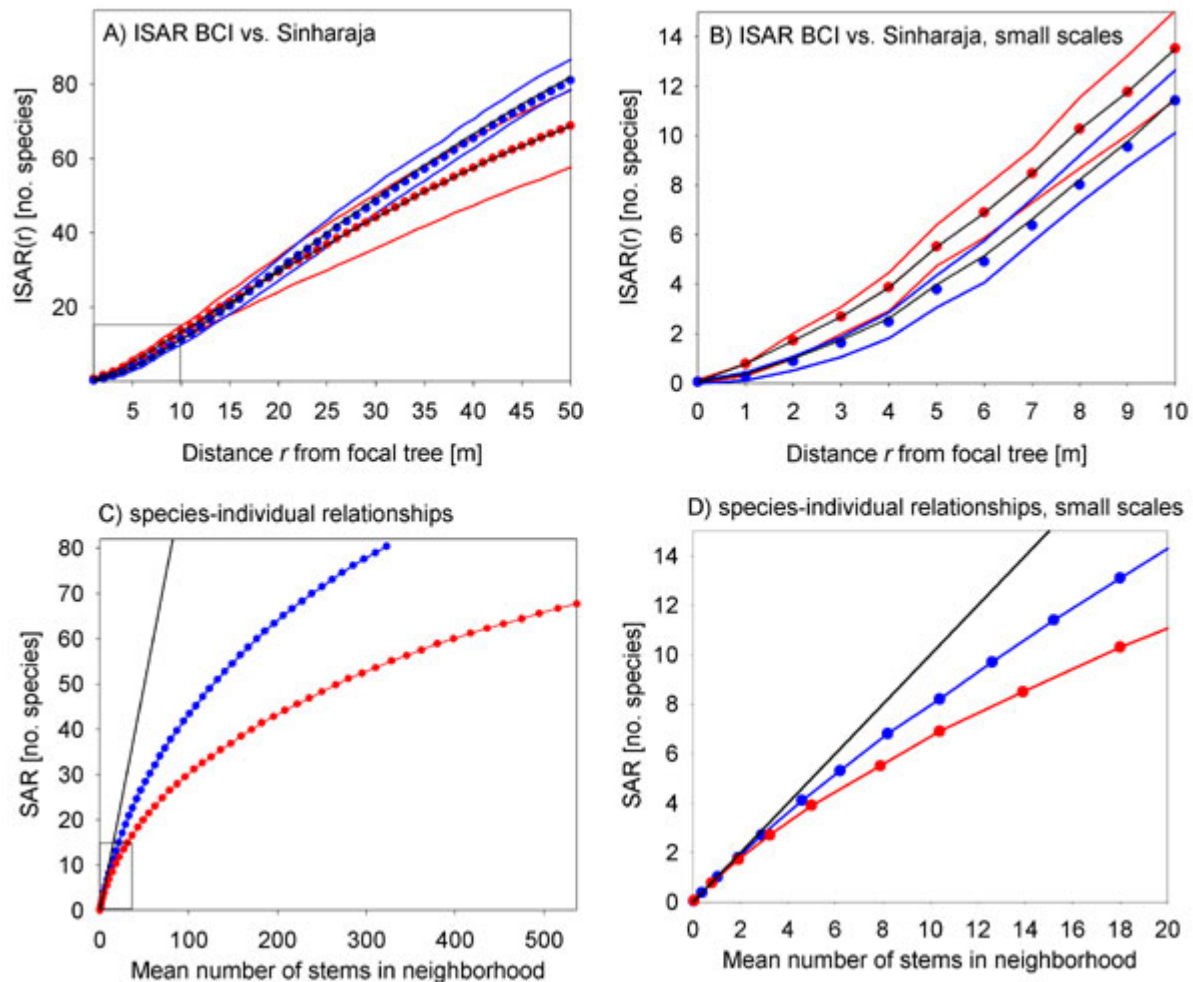


Fig. 4. Comparison of individual species-area relationships (*A* and *B*) and species-individual relationships (*C* and *D*) at BCI (blue) and Sinharaja (red) for different neighborhoods with radius r around the trees of the target species. The solid lines in *A* and *B* give the minimal and maximal observed values of all ISARs, respectively; the circles indicate the common SAR, and the black line indicates the average of all ISARs at a given plot. In *C* and *D*, the mean number of species in neighborhoods is plotted over the mean number of stems in these neighborhoods, and the black line is the 1-to-1 line.

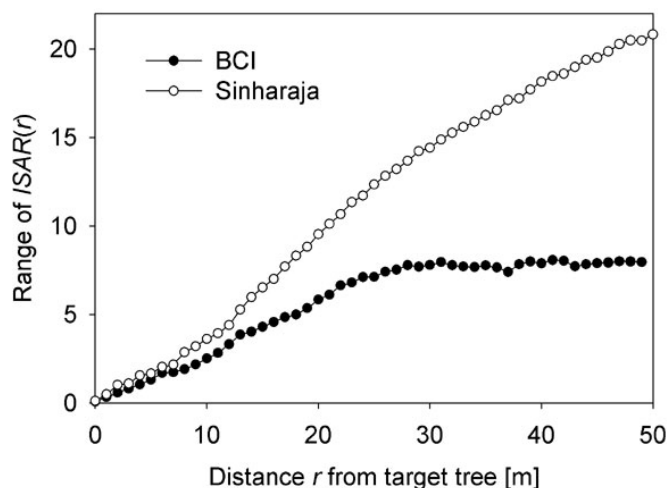


Fig. 5. The range of the individual species-area relationship at different distances r from the target tree. Note that the largest light gaps at BCI have a radius of ≈ 20 m.

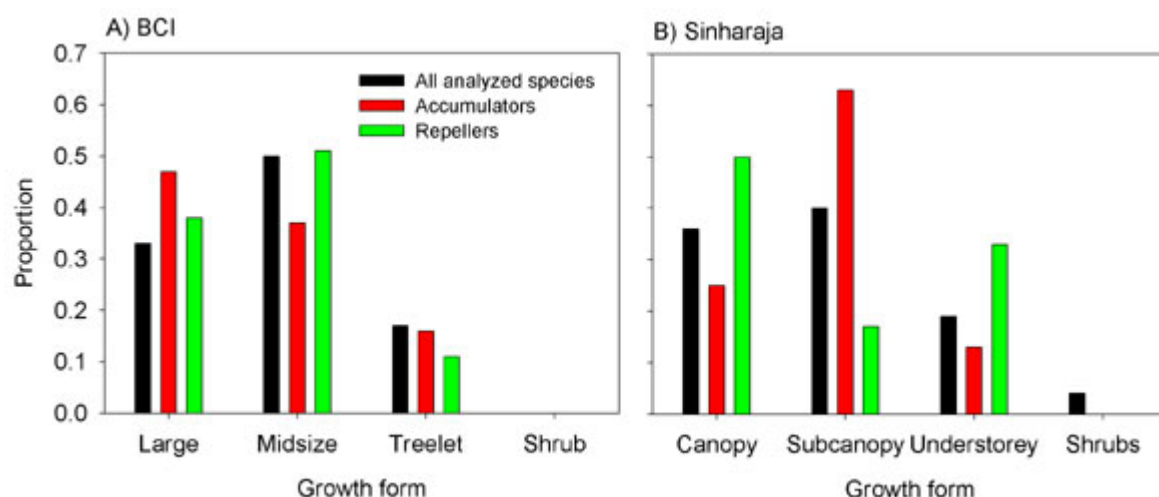


Fig. 6. Distribution of growth forms among accumulators and repellers. At BCI and Sinharaja, there were 22 and 12 species, respectively, with significant departure from the heterogeneous null model (as indicated by the goodness-of-fit test for scales 0-20 m). At BCI, six (at Sinharaja, eight) of these species acted at some scales as accumulators, twenty-one (at Sinharaja, six) as repellers, but five (at Sinharaja, two) acted as both accumulators and repellers. The graphs show the distribution of growth forms among all species analyzed (black bars), accumulators (red bars), and repellers (green bars). Trees at BCI were classified as large if they had a height >20 m, as subcanopy for 10-20 m, as understorey for 4-10 m, and as shrub for <4 m. The BCI classification data were taken from ref. 1. The classification data for Sinharaja were taken from ref. 2.

1. Condit R, Hubbell SP, Foster RB (1996) *J Trop Ecol* 12:231-256.

2. Gunatilleke CVS, Gunatilleke IAUN, Ethugala AUK, Esufali S (2004) *Ecology of Sinharaja Rain Forest and the Forest Dynamics Plot in Sri Lanka's Natural World Heritage Site* (WHT Publications, Colombo, Sri Lanka).

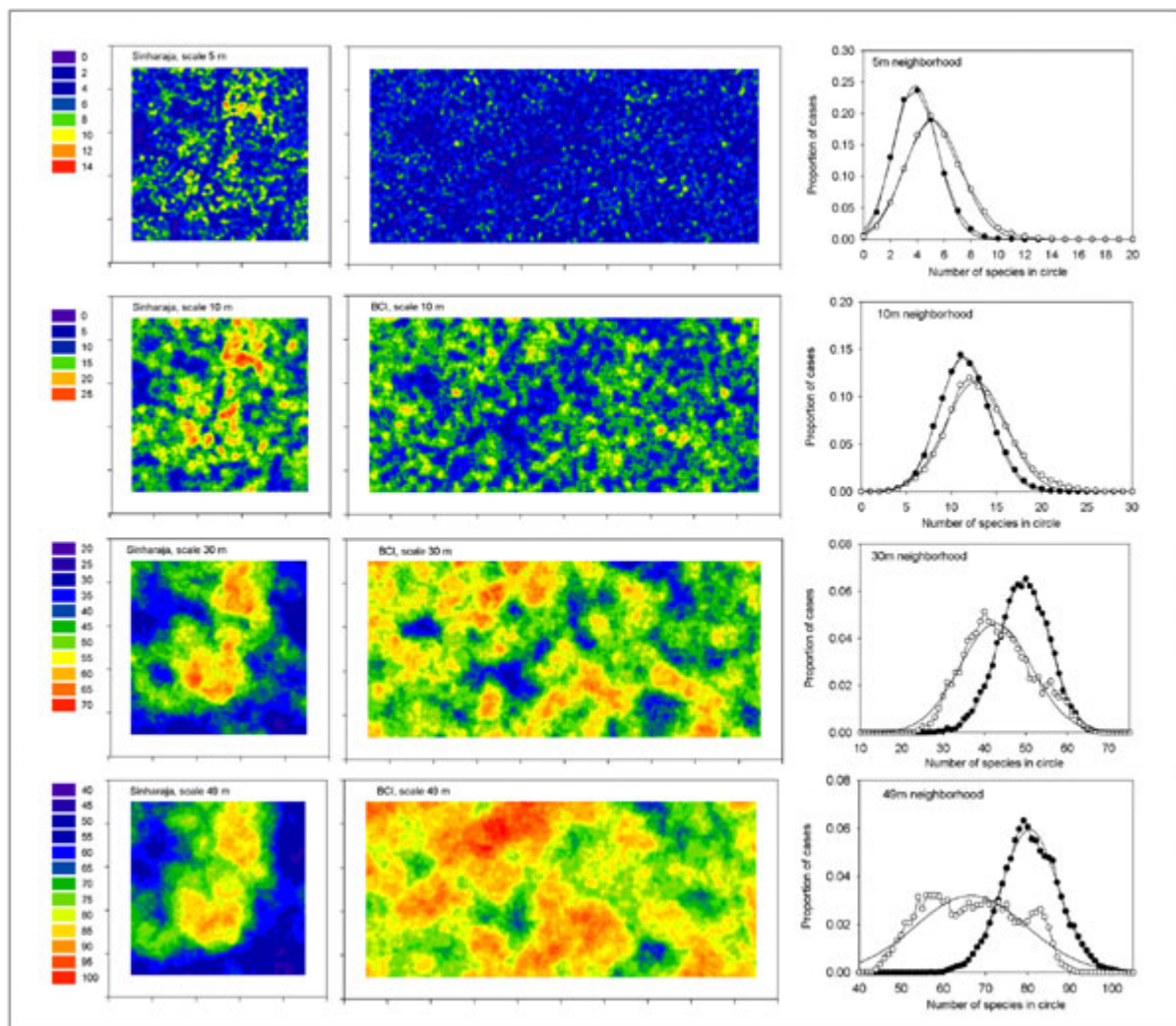


Fig. 7. Spatial variability of local diversity. The figures show the spatial variation in local diversity at neighborhoods of 5, 10, 30, and 49 m for Sinharaja (*Left*), and BCI (*Center*), and the distribution function of local diversity (*Right*) for Sinharaja (open circles) and BCI (filled circles). We sampled the number of species in circles with 5, 10, 30, and 49-m radii placed on the nodes of a 4×4 -m grid at the inner plot of each FDP (i.e., leaving a buffer of 50 m). The figures in *Right* show the distributions of the circles containing a given number of species and the fit with the normal distribution. The mean values \pm standard deviation at BCI are 3.9 ± 1.6 , 11.4 ± 2.8 , 49.5 ± 6.2 , and 80.5 ± 6.7 for the scales 5, 10, 30, and 49 m, respectively, and for Sinharaja 5.2 ± 2.0 , 12.7 ± 3.4 , 42.7 ± 8.7 , and 66.5 ± 13.2 , respectively. At BCI, the distribution function of the number of species in circular sampling areas followed, for all neighborhoods <50 m, almost perfect normal distributions. However, pronounced habitat heterogeneity at Sinharaja produced departures from normal distributions for neighborhoods >30 m, and large areas of below- and above-average diversity appear. The differences in local diversity are related to topography and differences in nutrient and moisture levels, vegetation structure, and gap dynamics at different elevations.

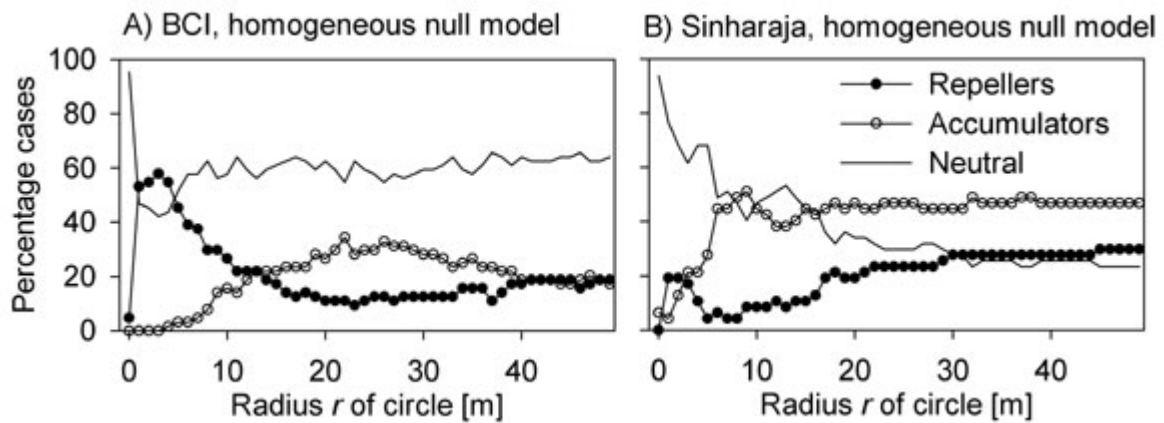


Fig. 8. Proportion of significant diversity repellents and accumulators at BCI and Sinharaja. (A) BCI using the homogeneous null model which does not account for potential habitat association. (B) Sinharaja using the homogeneous null model. The goodness-of-fit test applied for the interval 0-50 m revealed that 57% of all species at BCI and 79% of all species at Sinharaja behaved nonneutrally with respect to the homogeneous null model. The figure for BCI is somewhat surprising because this site was originally chosen in part so that habitat variation was minimal whereas habitat association was strong at the Sinharaja plot.

Table 1. Local dominance of the most clustered and underdispersed species, measured within 10-m neighborhoods

Species	n_t	Local stem numbers of target species $M_{tt}(r)$	Local stem numbers of other species $M_{to}(r)$	Cluster tendency of target species $\Delta_{tt}(r)$	Local dominance $D(r)$
BCI					
<i>Gustavia superba</i> *	375	4.71	13.7	4.33	0.256
<i>Socratea exorrhiza</i>	201	1.78	14.5	1.57	0.109
<i>Poulsenia armata</i> †	451	1.91	13.5	1.44	0.124
<i>Cecropia insignis</i> ‡	161	1.50	15.8	1.34	0.087
<i>Croton billbergianus</i>	62	1.26	12.9	1.19	0.089
<i>Trichilia tuberculata</i> †	1,302	2.47	12.6	1.12	0.164
<i>Miconia argentea</i>	56	1.07	15.0	1.01	0.067
<i>Guettarda foliacea</i>	46	0.00	15.4	-0.05	0.000
<i>Pterocarpus rohrii</i>	53	0.00	15.7	-0.05	0.000
<i>Tachigali versicolor</i>	65	0.00	14.7	-0.07	0.000
<i>Guapira standleyana</i>	73	0.00	15.0	-0.08	0.000
<i>Brosimum alicastrum</i> †	136	0.06	14.2	-0.08	0.004
Sinharaja					
<i>Agrostistachys hookeri</i>	129	7.71	23.9	7.40	0.244
<i>Mesua nagassarium</i> †	1,130	8.52	16.8	5.88	0.336
<i>Mallotus fucescens</i> †	64	5.53	20.3	5.38	0.214
<i>Garcinia hermonii</i>	1,154	7.42	21.6	4.73	0.255
<i>Syzygium neesianum</i>	167	3.29	21.1	2.90	0.135
<i>Shorea trapezifolia</i>	404	3.83	22.0	2.88	0.148
<i>Shorea worthingtonii</i> †	169	3.21	24.0	2.81	0.118
<i>Shorea cordifolia</i>	241	2.95	26.2	2.38	0.101
<i>Shorea megistophylla</i>	236	2.89	24.0	2.34	0.107
<i>Mesua ferrea</i> †‡	186	2.49	21.2	2.06	0.105

n_t , number of stems of the target species within the inner plot; $M_{tt}(r)$, average number of stems of the target species (symbolized by subscript t) within circles with radius $r = 10$ m and area $a(r)$ around the stems of the target species (not counting the focal stem); $M_{to}(r)$, average number of stems of all other species (symbolized by subscript o) within circles with radius r around the stems of the target species; λ_t , intensity of the target species within the inner plot. $\Delta_{tt}(r) = M_{tt}(r) - \lambda_t a(r)$ compares $M_{tt}(r)$ with the expected number of stems of the target species within area $a(r)$ and describes the tendency to clustering or regularity [if $\Delta_{tt}(r) > 0$, the species has a tendency to clustering and for $\Delta_{tt}(r) < 0$, the species has a tendency to regularity], and the local dominance of the target species is defined as $D(r) = M_{tt}(r) / [M_{tt}(r) + M_{to}(r)]$. For BCI, the most clustered and the most underdispersed species are shown, for Sinharaja, only clustered species are shown because at the 10-m scale, all study species had a tendency to clustering.

*The unusually high locally density of this species occurred in a disturbed area at the northern border of the plot.

†Species with significant departure from the heterogeneous null model, being repeller at some scales.

‡Species with significant departure from the heterogeneous null model, being accumulator at some scales.

SI Text

Implementation of Heterogeneous Poisson Null Model. To implement the heterogeneous null model, we first created a random pattern which was then thinned with the spatially varying intensity function $\lambda(x, y)$. To determine the intensity function of the stems of the target species, we used an Epanechnikov kernel that yields $e_h(d) = (3/4h)(1 - (d/h)^2)$ if $-h \leq d \leq h$ [and $e_h(d) = 0$ otherwise], where d is the distance from a focal stem, and h is the bandwidth (1). For a given location (x, y) , the intensity function $\lambda(x, y)$ is constructed by using a moving window with circular shape and radius h around location (x, y) and summing up all stems in the circle, but weighting them with factor $e_h(d)$ according to their distance d from the focal location (x, y) . We used a bandwidth of 50 m, thus all potential spatial structure in the pattern of the target species is removed below scales of 50 m. An algorithm to generate a heterogeneous Poisson process by thinning of a homogeneous Poisson process is e.g., available from the R package SpatStat (2). Below is the Delphi code of the algorithm used here, written in Pascal.

```
//Application of a heterogeneous Poisson null model to create a
//randomization of the pattern of target species

const // globally defined constants and variables
  dim1=500; //plot dimension in x-direction = 500m
  dim2=500; //plot dimension in y-direction = 500m
  RadiusMW=50; //Radius of moving window = 50m
  rmax=50; //buffer width for edge correction
  fpPoints=115; //Number of points of pattern of target species

focalpattern:array[1..115,1..2] of real = //Example for coordinates of
//target species
(( 247.0, 238.9), ( 371.6, 426.5), ( 69.9, 430.5), ( 165.1, 400.1),
( 193.7, 496.3), ( 378.7, 170), ( 321.3, 188.1), ( 219.5, 414.8),
( 488.3, 320), ( 298.1, 16.3), ( 160.1, 152.2), ( 261.6, 418.7),
( 304.2, 483.7), ( 204.7, 491.7), ( 326.2, 27.4), ( 155.4, 474.6),
( 223.4, 159.7), ( 289.2, 477.6), ( 53.9, 369.6), ( 405.1, 451.1),
( 173.5, 106.5), ( 264.9, 384), ( 163.1, 155.9), ( 133, 78.3),
( 134.1, 34.9), ( 17.3, 432.7), ( 330.5, 123.4), ( 64.7, 410.1),
( 95.8, 100.9), ( 204.7, 249), ( 486.3, 10.4), ( 170.3, 187.9),
( 201.6, 495.4), ( 258.3, 331.5), ( 365.5, 460.7), ( 136, 444.3),
( 382.3, 411.8), ( 313.1, 436.7), ( 276.1, 47.2), ( 327.6, 246.9),
( 129, 51.2), ( 387.6, 264.1), ( 145.2, 144.5), ( 310, 432),
( 62.8, 370.8), ( 92.5, 405.4), ( 45.4, 134.2), ( 407.7, 425.2),
( 106.9, 32.6), ( 184.4, 66.1), ( 138.4, 371.8), ( 285.1, 134.5),
```

```
( 121.5, 71.7), ( 289.2, 327.7), ( 116.5, 18.2), ( 462.4, 102.2),
( 51, 164.8), ( 358.6, 199.2), ( 124.2, 74.3), ( 360.8, 164.8),
( 332.6, 233.1), ( 310.2, 56.2), ( 100.3, 198.4), ( 134.7, 63.8),
( 45.8, 373.4), ( 131.1, 433.5), ( 416.3, 440.3), ( 370.9, 203.3),
( 466.4, 109.6), ( 277.6, 83.3), ( 364.8, 203.8), ( 93.7, 40.9),
( 310.9, 264.9), ( 8.7, 387.5), ( 324.1, 110.7), ( 258.3, 309.4),
( 352.9, 214.7), ( 353.2, 145.9), ( 413, 435.8), ( 302.8, 435.1),
( 341.6, 179.4), ( 263, 286.2), ( 387, 254.8), ( 439, 261.4),
( 294.1, 437.6), ( 352.5, 142), ( 175.6, 390), ( 110.2, 81.4),
( 185.2, 211.9), ( 339.9, 36), ( 306.5, 137.3), ( 167.3, 146.1),
( 331.8, 229.8), ( 454.2, 220.5), ( 348.9, 336.3), ( 258.5, 484),
( 304.3, 118.4), ( 132, 34.8), ( 72, 46.2), ( 358.5, 205.6),
( 266.7, 74.2), ( 352.8, 275.9), ( 253.8, 81.9), ( 283.3, 64.7),
( 375.1, 165.8), ( 368.8, 161.5), ( 305.1, 239.6), ( 15.9, 388),
( 161.3, 70.4), ( 182.7, 103.2), ( 186.2, 45.2), ( 109, 2.4),
( 371.3, 254.2), ( 38.5, 121.1), ( 109.6, 428.6));
```

```
Function rangex(x:integer):byte;
```

```
var
```

```
range:byte;
```

```
begin
```

```
range:=1;
```

```
if x<=0 then range:=0;
```

```
if x>dim1 then range:=0;
```

```
rangex:=range;
```

```
end;
```

```
Function rangey(x:integer):byte;
```

```
var
```

```
range:byte;
```

```
begin
```

```
range:=1;
```

```
if x<=0 then range:=0;
```

```
if x>dim2 then range:=0;
```

```
rangey:=range;
```

```
end;
```

```
Function Kernel(h,x:real):real; //the Epanechnikov kernel
```

```
begin
```

```
Kernel:= (3/(4*h))*(1 - x*x/(h*h));
```

```
end;
```

```
//-----The procedure HeterogeneouPoisson creates a point pattern from a
//heterogeneous
```

```
// Poisson process based on the pattern of the target species
```

```
Procedure HeterogeneouPoisson;
```

```
var
```

```
PatternNullModell:array[1..fpPoints,1..2] of integer; //Pattern
```

```
//created with null model
```

```
lambda:array of array of single; //--the estimated intensity of pattern
//of target species at (x,y)
```

```
pattern:array of array of byte; //--grid representation of pattern of
//target species
```

```
i1,i2,j1,j2,anzp1,i,x1,y1,anz1,nr,zahl:integer;
```

```
lmax,dist:real;
```

```
datei:textfile;
```

```

begin
  setlength(lambda,dim1+2,dim2+2);
  setlength(pattern,dim1+2,dim2+2);

  //-----First step, calculation of intensity lambda of pattern of
  //target species

  for i1:=0 to dim1+1 do
    begin
    for i2:=0 to dim2+1 do lambda[i1,i2]:=0;
    end;

    //read pattern of target species and convert it into a 1m x1m grid
    anzP1:=0;
    for i:=1 to fpPoints do
      begin
      x1:=1+trunc(focalPattern[i,1]);
      y1:=1+trunc(focalPattern[i,2]);
      pattern[x1,y1]:= pattern[x1,y1]+1;
      anzP1:=anzP1+1;
      end;

      //Kernel estimate of intensity using a moving window
      //the moving window visits all points in the inner plot
      for i1:=1 to dim1 do
        begin
        for i2:=1 to dim2 do
          begin
          anz1:=pattern[i1,i2]; //--anz1 points within cell (i1,i2), the j1-j2
          //slope calculates
          // the contribution of these points to the intensity at cell
          if anz1>0 then // (i1+j1,i2+j2)
            begin
            for j1:=-RadiusMW to RadiusMW do
              begin
              for j2:=-RadiusMW to RadiusMW do
                begin
                dist:=sqrt(j1*j1+j2*j2);

                if ((dist<=radiusMW) and (rangex(i1+j1)=1) and (rangey(i2+j2)=1)) then
                  begin
                  lambda[i1+j1,i2+j2]:=lambda[i1+j1,i2+j2]+anz1*Kernel(RadiusMW,dist);
                  end;
                end;
              end;
            end;
          end;
        end;
      end;

      //normalize intensity
      lmax:=0;
      for i1:=1 to dim1 do
        begin
        for i2:=1 to dim2 do
          begin

```

```

if lambda[i1,i2]>lmax then lmax:=lambda[i1,i2];
end;
end;
for i1:=1 to dim1 do
begin
for i2:=1 to dim2 do lambda[i1,i2]:=lambda[i1,i2]/lmax;
end;

//--random points within inner rectangle ((rmax,dim1-rmax),(rmax,dim2-
//rmax))
//--are randomly thinned with intensity lambda
nr:=1;
while nr<=anzP1 do
begin
x1:=rmax+trunc(random(dim1-2*rmax));
y1:=rmax+trunc(random(dim2-2*rmax));
zahl:=random(1000);
if zahl<1000*lambda[x1,y1] then
begin
PatternNullModell[nr,1]:=x1;
PatternNullModell[nr,2]:=y1;
nr:=nr+1;
end;
end;

//output of intensity in ArcView ASCII format
assignfile(datei,'intensity.asc');
rewrite(datei);
writeln(datei,'ncols 500');
writeln(datei,'nrows 500');
writeln(datei,'xllcorner 1');
writeln(datei,'yllcorner 1');
writeln(datei,'cellsize 1');
writeln(datei,'NODATA_value -9999');
for i1:=1 to dim1 do
begin
for i2:=1 to dim2 do
begin
writeln(datei,lambda[i1,i2]:6:5);
end;
end;
closefile(datei);

//output of pattern created with heterogeneous Poisson null model
assignfile(datei,'nullmodel.txt');
rewrite(datei);
for nr:=1 to anzP1 do
begin
writeln(datei,PatternNullModell[nr,1]:5,' ',
PatternNullModell[nr,2]:5);
end;
closefile(datei);
end;

```

1. Stoyan D, Stoyan H (1994) *Fractals, Random Shapes and Point Fields* (Wiley, New York).

2. Baddeley A, Turner R (2005) *Journal of Statistical Software* 12:1-42.